Desalination and Water Treatment
www.deswater.com
doi: 10.5004/dwt.2022.28802

275 (2022) 103–115
November

Removal of Helaktyn Blue F-2R via adsorption onto modified post-coagulation sludge

Barbara Pieczykolan*, Patrycja Krzyżowska

Department of Water and Wastewater Engineering, Faculty of Energy and Environmental Engineering, The Silesian University of Technology, 18 Konarskiego Str., 44-100 Gliwice, Poland, emails: barbara.pieczykolan@polsl.pl (B. Pieczykolan), pat.krzyzowska@gmail.com (P. Krzyżowska)

Received 28 February 2022; Accepted 27 July 2022

ABSTRACT

In the study, post-coagulation sludge was used in the sorption of the Helaktyn Blue F-2R. The sludge was subjected to: (1) drying, or (2) combusting, either (3) oxidizing with H_2O_2. The effect of pH, the effect of the contact time (and examining the adsorption kinetics), and the adsorption isotherm were examined. The parameters of selected models of adsorption isotherms (Freundlich, Langmuir, Jovanovic, Dubinin–Radushkevich, Sips, and Toth) were determined using nonlinear estimation. In the case of all sorbents strong acidic conditions were required for the adsorption process occurrence (pH 2). According to the sorption kinetics, for all sorbents, the pseudo-first-order model were matching the most to the experimental results, which suggests that the physisorption process occurred. Based on the examination of the intraparticle diffusion model, it can be concluded that the rate of the adsorption process was controlled to a greatest extent by the inner diffusion process than by the film diffusion process. The values of *C* for all sorbents in the intraparticle diffusion model were positive and greater than 0, which indicates that the intraparticle diffusion was not only the rate-controlling step. Based on the examination of different isotherms' models, the greater sorption capacity was obtained for dried sludge, a little less for the oxidized sludge, and the smallest for combusted sludge. Moreover, the results indicate that the sorbent produced from combusted sludge had the greatest surface heterogeneity, while the lowest – the sorbent obtained from dried sludge.

Keywords: Sorption process; Dye adsorption; Kinetics adsorption; post-coagulation sludge; Adsorption isotherm

1. Introduction

Coagulation is one of the most frequently used technological processes in the treatment of surface water. The reagent (called a coagulant) introduced into the treated water leads to the formation of a flocculent suspension as a result of a series of chemical reactions. This process removes colloidal particles, suspended solids, compounds that cause water turbidity and color, as well as organic compounds from the water. The sludge is characterized by an amorphous structure with a significantly developed specific surface. It is mainly composed of metal hydroxides precipitated from alum or iron reagents used in the coagulation process. The characteristics and properties of post-coagulation sludge depend on the treatment technology used and the physicochemical composition of the treated water. This sludge mainly consists of water (hydration level up to 98% and above). In classical systems, the management of sludge, generated in the coagulation process, includes thickening, conditioning (with the possible recovery of aluminum compounds), dewatering, and final disposal [1–3].

* Corresponding author.

Presented at the 2nd International Conference on Strategies toward Green Deal Implementation – Water, Raw Materials and Energy (ICGreenDeal2021), 8–10 December 2021, held online by the Mineral and Energy Economy Research Institute, Polish Academy of Sciences

1944-3994/1944-3986

In recent years, research has been conducted on the use of residuals from water treatment in the production of building materials. De Carvalho Gomes et al. [4] used sludge from water purification by coagulation where ferric chloride as a coagulant was applied. In their research, the water treatment sludge was subjected to the pyrolysis process at 700°C, and then it was used as a cement admixture to obtain cement composites. Another example of using sludge from water treatment as an additive to building materials is an attempt to produce clay-free bricks [5]. In these studies, sludge from water treatment was used to produce clay-free bricks as the only ingredient in bricks but also in a mixture with glass powder and marble waste. Other studies showed that residuals from water treatment and waste bricks were used to produce new bricks [6]. Benlalla et al. [7] also used sludge from water treatment as complementary material to make ceramic bricks. In this case, the sludge came from a water treatment plant where the coagulation process was carried out with aluminum sulfates and cationic polyelectrolytes. Gomes et al. [8] used the sludge from the coagulation of water with iron chloride to produce cement paste.

There are also experiments aimed at using water treatment residuals as a sorbent. An example may be the production of granulated sorbent prepared by mixing chitosan with sludge (generated during the iron and manganese removal process) to remove arsenic(V) [9]. Another example is the removal of perchlorate by using sorbent made from the residual from drinking-water treatment. In that case, the sludge was generated during the treatment process where aluminum coagulant with a small amount of a copolymer of sodium acrylate and acrylamide were used [10].

Other waste materials can also be used to form adsorbents. Currently, a relatively wide range of research has been carried out on the use of sewage sludge as sorbent. Usually, sewage sludge is physically or chemically activated and then used in an adsorption process. An example may be the use of chemical-activated sewage sludge with $ZnCl_2$ and H_2SO_4, followed by pyrolysis at 450°C in a nitrogen atmosphere [11]. Liu et al. [11] used this sludge to adsorb the dye Reactive Brilliant Red X-3B. Björklund and Li [12] used the activated sludge collected from the oxygen chamber of the municipal sewage treatment plant in their research. First, they used the chemical activation of the sludge with $ZnCl_2$ and then subjected it to the pyrolysis process at 500°C. The prepared sludge-based activated carbon was used as a sorbent to remove eight hydrophobic organic compounds frequently detected in stormwater. Rozada et al. [13] used anaerobically digested sewage sludge. They chemically activated this pellet with H_2SO_4 and then pyrolysed it under nitrogen at 625°C. The sorbent prepared in this way was used in the process of adsorption of methylene blue and saphranine dyes. In studies conducted by Pieczykolan and Płonka [14] the excess activated sludge was dried and grounded into powdered form and used for adsorption of two dyes: Acid Red 18 and Acid Green 16. Magnetite nanoparticles, which were produced by the chemical co-precipitation method and then modified [15], were also used to remove the Acid Red 18 dye in the adsorption process. Whereas Ali et al. [16] produced activated carbon from pomegranate peel coated with zero-valent iron nanoparticles (nZVI). This sorbent was used for amoxicillin from an aqueous solution.

The publication describes the results of experiments on the use of the sludge (formed during water treatment by coagulation) in the adsorption process of the Helaktyn Blue F-2R. The post-coagulation sludge was subjected to thermal and/or chemical processes, as a result of which three different types of waste sorbents were obtained. In the studies described so far, few studies have been carried out on the use of residuals from water treatment processes to produce sorbets. Therefore, it was decided to use the sediment formed in the water treatment process for the adsorption of the dye. Moreover, so far no one has used in their research the methods of post-coagulation sludge preparation to produce sorbents that were used in the experiments described in this article.

2. Materials and methods

Sorption studies were carried out in a batch system using waste sorbents to adsorb the Helaktyn Blue F-2R (Boruta-Zachem, Poland).

2.1. Dye characteristic

Helaktyn Blue F-2R, called Reactive Blue 81 (C.I.18245, CAS 75030-18-1), with molecular weigh 808.49 and molecular formula $C_{25}H_{14}Cl_2N_7Na_3O_{10}S_3$ [17] was used in the experiments. It is a dye belonging to the group of reactive dyes, the single azo class, which has groups such as chlorotriazine or epoxy in their molecules, which form a permanent bond with the fibers of dyed fabrics [18]. It is used for cotton fabrics, polyamide, wool dyeing, or fountain of rolling dyeing [17]. The chemical structure of the Helaktyn Blue F-2R is given in Fig. 1.

This dye contains three sulfonate groups, the dichlorotriazine, ring, and also the azo-group which connects to phenyl and naphthyl [19].

2.2. Sorbents preparation and their characteristics

Post-coagulation sludge from a surface water treatment plant coagulant was used as a waste sorbent. During the water treatment, the volumetric coagulation/flocculation process with the use of aluminum sulphate was applied. The sludge was characterized by a dry matter concentration of 11.5 g/kg, a dry mineral matter content of 49.0%, and a dry organic matter content – of 51.0%. The hydration of the used sludge was 99.8%.

The sludge, which was generated during the water treatment process, was separated from the treated water and subjected to a thickening process. Then, under laboratory conditions, the sludge was processed in three different ways, resulting in the production of three types of waste sorbents used in this study.

In the first case, the thickened sludge was dried to the constant weight at 105°C in a laboratory drier and then ground to a grain fraction <0.49 mm.

In the case of the second method, the sludge was dried, ground to a grain fraction <0.49 mm, and then combusted in a muffle furnace at 300°C for 60 min.

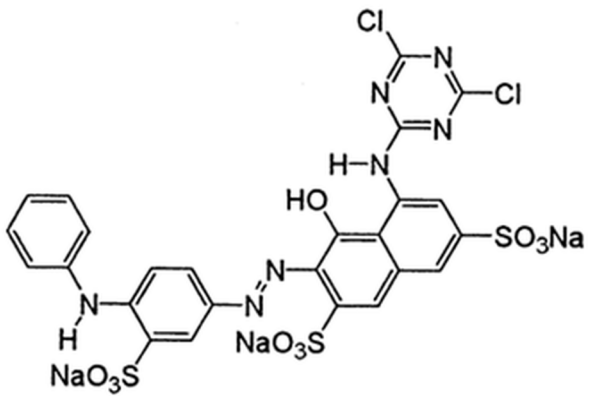

Fig. 1. Structural formula of dye Helaktyn Blue F-2R [17].

In the last case, the dried and ground sludge was oxidized with hydrogen peroxide. For this purpose, in an aqueous medium, the post-coagulation sludge was treated with H_2O_2 in the dose of 0.42 g H_2O_2/g of sludge for 24 h, then the sludge was washed with distilled water and dried again.

For all three types of sorbents, microscopic images were taken using the stereoscopic light microscope SteREO Discovery by ZEISS. For examination of the structure of the surface of each sorbent, the Brunauer–Emmett–Teller (BET) surface area, total pore volume, and average pore size diameter were determined. For this purpose, the N_2 adsorption at 77 K was conducted (by using Gemini VI of Micromeritics USA).

Moreover, the Fourier-transform infrared spectroscopy (FTIR) measurement of sorbents was made using the Thermo Scientific™ FTIR Nicolet™ iS50 spectrometer, which allows for the identification of chemical bonds and functional groups present in the tested material. The study with the Fourier transforms infrared spectroscope was carried out in the ATR (Attenuated total reflection) mode, which allowed to record of the transmittance spectrum as a function of the wavenumber in the range from 400 to 3,500 cm^{-1}.

2.3. Adsorption methodology

The batch sorption experiments were conducted in three stages: (1) determination of the reaction pH; (2) determining the impact of contact time; (3) determination of the adsorption isotherm.

In the case of the first stage of the studies, the effectiveness of the sorption process was determined using five different pH values: 2, 4, 6, 8, and 10 when the constant concentration of the dye (C_0 = 700 mg/dm^3), the constant amount of sorbents (2 g/dm^3) and a constant contact time were used. For this purpose, 50 cm^3 of a dye solution with a defined concentration and an adjusted pH value were introduced into a 250 cm^3 conical flask (the pH was adjusted with either 50% H_2SO_4 or 5% NaOH). To the sample prepared in this way, 0.1 g of sorbent was added and the whole was shaken on a laboratory shaker (GFL model 3005) for a specified time. Then the sorbent was separated from the dye solution and the concentration of the remaining dye was determined by the spectrophotometric method with the use of a standard curve. The absorbance measurement was performed on the WTW SpectroFlex 6100 spectrophotometer. Based on the measurement of the concentration after the process and the value of the initial dye concentration, the amount of dye adsorbed by the unit mass of the sorbent was calculated [Eq. (1)].

$$q_e = \frac{(C_0 - C_e)}{m_{sl}} \tag{1}$$

where q_e is the amount of dye adsorbed (mg/g), C_e is the dye concentration at equilibrium (mg/dm^3), C_0 is the initial dye concentration (mg/dm^3), m_{sl} is the amount of sludge (g/dm^3).

In the second stage of the study, the experiments were carried out at a constant concentration of the dye (C_0 = 700 mg/dm^3), the constant amount of adsorbent (m_{sl} = 2 g/dm^3) and at the constant pH (determined in the first stage of the research) using different contact times ranging from 5 to 120 min. The procedure for conducting the tests was the same as in the first part.

To examine the mechanism of the adsorption process three types of kinetic models were used: pseudo-first-order [Eq. (2)] [20], pseudo-second-order (eq. 3.) [21], and intraparticle diffusion (eq. 4) [22]. To determine the parameters of pseudo-first-order and pseudo-second-order models, a nonlinear estimation was conducted by minimizing the RMSE (eq. 5) and chi-square (eq. 6) errors. For this purpose, the MS Office 365 Solver add-in was used. For the determined parameters, the R^2 values were calculated. The value of this coefficient gives information about the strength of the fitting of a kinetic model to the obtained experimental results.

In the case of the intraparticle diffusion model, the parameters were calculated using linear regression by the linear plot q_t vs. $t^{0.5}$. The K_{IPD} value was obtained from the slope of the regression line, and the C value was obtained from the intercept of the regression line [23].

$$q_t = q_e \cdot \left(1 - \exp\left(-k_1 \cdot t\right)\right)\left[\frac{\text{mg}}{g}\right] \tag{2}$$

$$q_t = \frac{q_e^2 \cdot k_2 \cdot t}{1 + q_e \cdot k_2 \cdot t}\left[\frac{\text{mg}}{\text{g}}\right] \tag{3}$$

$$q_t = K_{IPD} \cdot t^{0.5} + C \tag{4}$$

$$\text{RMSE} = \sqrt{\frac{1}{n-2}\sum_{i=1}^{n}\left(q_{e,\text{exp}} - q_{e,\text{calc}}\right)_i^2} \tag{5}$$

$$\chi^2 = \sum_{i=1}^{n}\frac{\left(q_{e,\text{exp}} - q_{e,\text{calc}}\right)_i^2}{q_{e,\text{calc}}} \tag{6}$$

where q_t is the amount of dye adsorbed after each contact time (mg/g), q_e is the amount of the adsorbed dye at equilibrium state (mg/g), k_1 is the rate constant of the pseudo-first-order equation (1/min), k_2 is the constant rate of the pseudo-second-order equation (g/(mg·min)), t is the contact time (min), $q_{e,\text{exp}}$ is the amount of dye adsorbed during the experiments (mg/g); $q_{e,\text{cal}}$ is the estimated value of amount of

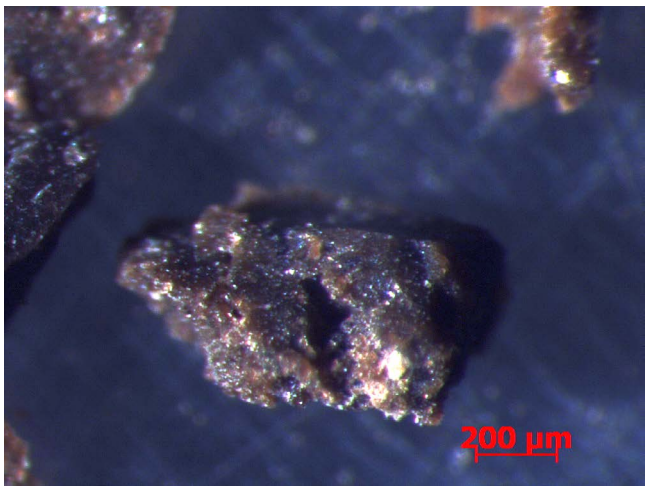

Fig. 2. Microscopic image of dried sludge.

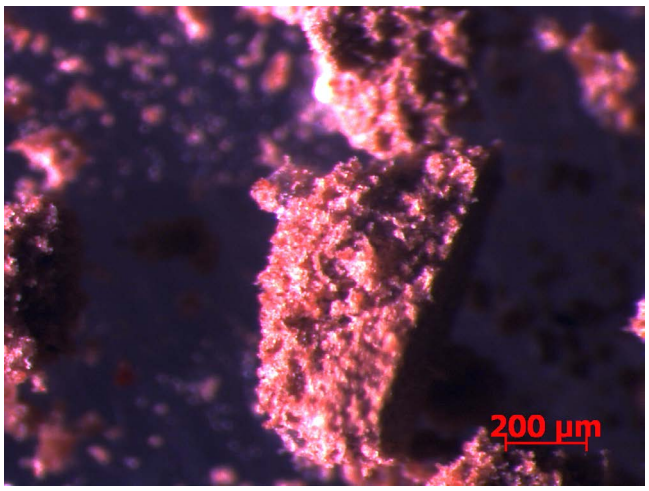

Fig. 3. Microscopic image of H_2O_2 oxidized sludge.

dye adsorbed (mg/g); K_{IPD} is the intraparticle diffusion rate constant (mg/(g·min$^{0.5}$)); C a constant depicting the boundary-layer effects (mg/g).

In the third stage, for the adjusted pH of the reaction and the contact time (in the second stage), a constant amount of sorbent was used, changing the initial concentration of the dye. Based on the results obtained at this stage of the tests, graphs of the adsorption isotherms were made for each sorbent. Moreover, parameters of selected models of adsorption isotherms were calculated. Six different models were used: four two-parameter (Freundlich, Langmuir, Jovanovic, and Dubinin–Radushkevich) and two three-parameter (Sips and Toth). To determine the parameters of isotherms, nonlinear estimation was used by minimizing the RMSE error [Eq. (5)] and chi-square error [Eq. (6)] using the Microsoft Office 365 Solver add-in.

All of the isotherm' models, their formulas, and parameter definitions are included in Table 1.

3. Results and discussion

3.1. Characteristic of adsorbents

3.1.1. Microscopic images

For all three types of sorbents, microscopic photos were taken using a stereoscopic light microscope. The analysis of these images shows that the lowest grain surface roughness was obtained for the sludge combusted at 300°C (Fig. 4). In the photo, the surface is slightly undulating and the smoothest. In the case of the sorbent obtained from the dried sludge, the surface of the grains is a bit more porous and folded than in the case of the combusted sludge (Fig. 2). The most developed surface of the grains was observed in the case of the sorbent obtained by oxidizing the sludge with hydrogen peroxide (Fig. 3). In this case, the surface is very varied and undulating.

Such significant differences in the morphological structure of the obtained sorbents may affect the effectiveness of the adsorption process. In the case of sorbents, their surface must be strongly unfolded and corrugated because it increases the value of the specific surface area of sorbents, expressed in m^2/g of sorbent.

3.1.2. FTIR measurements

FTIR measurement was also conducted for tested sorbents. The transmittance graphs in the range from 400 to 3,500 cm^{-1} of the wavenumber for each sorbent are shown in Fig. 5.

The obtained results of FTIR measurement indicate that the sorbent made of dried sludge had the highest humidity (water content – a wide transmittance band in the wavenumber range from 3,100 to 3,500 cm^{-1}). This is evidenced by the occurrence of the smallest transmittance values in this wavenumber range (Fig. 5). The sludge oxidized with H_2O_2 (Fig. 5) was characterized by a slight amount of humidity – as evidenced by the low absorbance value in this wavenumber range. On the other hand, the sorbent obtained from the combusted sludge was characterized by the lack of water in its structure (Fig. 5). For all sorbents, the transmittance peak at the wavelength of 2,360 and 2,340 cm^{-1} was recorded. This proves the presence of triple bonds on the sorbent surface (groups with C≡C or C≡N bonds). The highest peak at both of those wavelengths was measured for the sorbent produced by oxidation of the post-coagulation sludge. Moreover, for all tested sorbents, transmittance peaks in the range of wavenumber 1,456–1,558 cm^{-1} were also noted. This indicates the presence of O–H and C=N bonded groups. Besides, also for all sorbents, there were transmittance peaks at a length of 668 cm^{-1}. This again indicates the presence of the O–H groups or halogen compounds (C–Cl, C–Br, or C–I). In the case of the sorbent oxidized with H_2O_2, a wide transmittance band was noted in the wavenumber range from 1,000 to 1,100 cm^{-1}. Such a band may indicate the presence of C–O or C–O–C groups on the sorbent's surface [24–26].

3.1.3. Textural characterization

Based on the measurements of the specific surface and the porous structure of the tested sorbents, it can be

Table 1
Isotherm' models

Isotherm model	Nonlinear formula	Definitions of parameters
Freundlich	$q_e = K_F \cdot C_e^{1/n}$	q_e is the amount of dye adsorbed per gram of the adsorbent at equilibrium (mg/g); C_e is the equilibrium dye concentration (mg/dm^3); K_L is the Langmuir isotherm constant (dm^3/mg); q_m is the maximum monolayer coverage capacity in Langmuir model (mg/g); n is the Freundlich isotherm constant related to the heterogeneity of the process (–); K_F is the Freundlich isotherm constant connected with relative adsorption capacity; Q_s is the theoretical isotherm saturation capacity in Dubinin–Radushkevich model (mg/g); K_{DR} is the Dubinin–Radushkevich model constant related to the adsorption energy (mol^2/kJ^2); E is the average free energy adsorption (kJ/mol); ε is the Polanyi adsorption potential; R is the universal gas constant; T is the temperature (K); K_J is the Jovanovic isotherm constant related with adsorption energy (dm^3/g); q_{max} is the maximum adsorption capacity in the Jovanovic model (mg/g); q_{mS} is the saturation adsorption capacity in Sips model (mg/g); K_S is the Sips isotherm constant parameter related to adsorption energy; SP is the Sips isotherm exponent related to the heterogeneity of the surface (–); q_{mT} is the maximum monolayer coverage capacity in the Toth model (mg/g); K_T is the Toth isotherm constant parameter related to adsorption energy; t is the Toth isotherm exponent related to the heterogeneity of the surface (–).
Langmuir	$q_e = \frac{q_m \cdot K_L \cdot C_e}{1 + K_L \cdot C_e}$	
Jovanovic	$q_e = q_{max} \cdot \left[1 - \exp\left(-K_J \cdot C_e\right)\right]$	
Dubinin–Radushkevich	$q_e = Q_s \cdot \exp\left(-K_{DR} \cdot \varepsilon^2\right)$ $\varepsilon = RT \cdot \ln\left(1 + \frac{1}{C_e}\right)$ $E = \frac{1}{\sqrt{2 \cdot K_{DR}}}$	
Sips	$q_e = \frac{q_{mS} \cdot K_S \cdot C_e^{SP}}{1 + K_S \cdot C_e^{SP}}$	
Toth	$q_e = \frac{q_{mT} \cdot K_T \cdot C_e}{\left(1 + \left(K_T \cdot C_e\right)^t\right)^{1/t}}$	

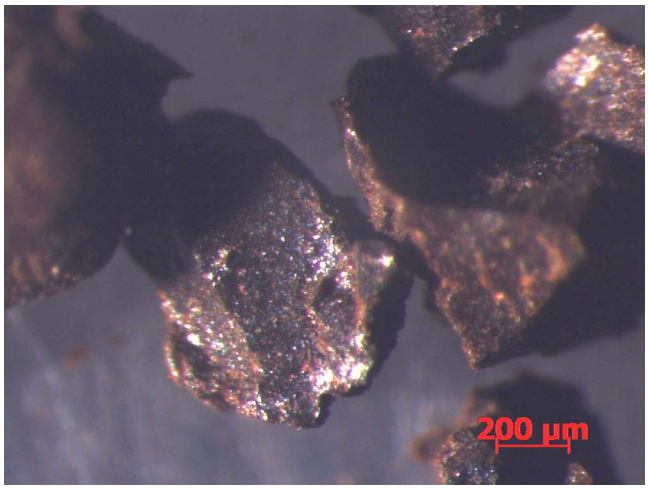

Fig. 4. Microscopic image of combusted sludge.

concluded that the largest value of BET surface, as well as Barrett–Joyner–Halenda (BJH) adsorption cumulative surface area of pores between 0.1000 and 300.0000 nm diameter and BJH desorption cumulative surface area of pores between 0.1000 and 300.0000 nm diameter, was obtained for the sorbent generated from the dried of post-coagulation sludge (Table 2). Slightly lower values of those parameters were obtained for the sorbent made of dried and oxidized with H_2O_2 sludge. In the case of the last third sorbent (obtained from the combustion of the post-coagulation sludge), the values of the BET surface area and the cumulative surface area of pores were several times lower than in the case of dried sorbent. Also, in the case of cumulative volume pores between 0.1000 and 300.0000 nm in diameter, the highest values were measured for the sorbent made from the dried sludge and made from the oxidized sludge. In the case of the last one, values of these parameters were again several times lower than for the other ones. However, in the case of the average pore size diameter for all three sorbents, the obtained values were similar, ranging from 3.4056 to 5.1152 nm in the case of the BJH adsorption and BJH desorption method. In the case of adsorption average pore width (4V/A by BET), these values ranged from 1.81785 to 1.85812 nm. Therefore, the conducted analysis shows a significant influence of the combustion process on the porous structure and the size of the specific surface area. The combustion of the sludge contributed to decreasing the porous structure of the sorbent and therefore to decrease the specific surface area.

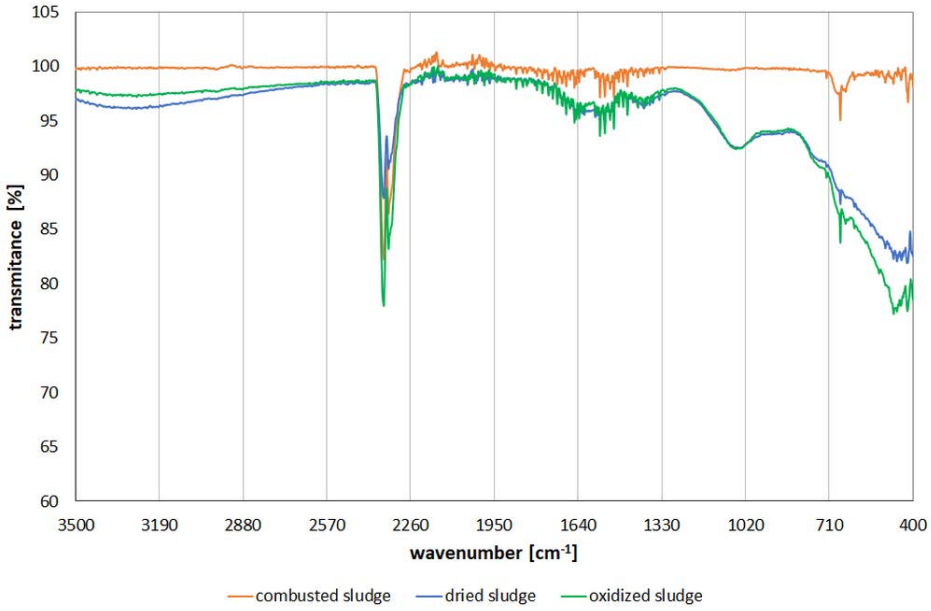

Fig. 5. FTIR measurement for sorbents.

Table 2
Structural characteristics of sorbents

Parameter	Type of sorbent		
	Dried sludge	Combusted sludge	Sludge oxidized with H_2O_2
BET surface area, m^2/g	66.4489	8.4885	58.7946
BJH adsorption cumulative surface area of pores between 0.1000 and 300.0000 nm diameter, m^2/g	151.9	31.516	148.154
BJH desorption cumulative surface area of pores between 0.1000 and 300.0000 nm diameter, m^2/g	154.959	21.886	115.6152
BJH adsorption cumulative volume of pores between 0.1000 and 300.0000 nm diameter, cm^3/g	0.161176	0.026833	0.189458
BJH desorption cumulative volume of pores between 0.1000 and 300.0000 nm diameter, cm^3/g	0.183164	0.026733	0.203849
Adsorption average pore width (4V/A by BET), nm	1.83935	1.81785	1.85812
BJH adsorption average pore diameter (4V/A), nm	4.2443	3.4056	5.1152
BJH desorption average pore diameter (4V/A), nm	4.7281	4.8867	7.0527

The obtained measurements of the sorbents' structure correlate with the obtained microscopic image, where the most diverse surface was observed in the case of the sorbent produced from the dried post-coagulation sludge and the one made from oxidizing the sludge.

3.2. Effect of pH

The conducted tests showed that for all types of sorbents, the adsorption process of Helaktyn Blue F-2R occurred only at pH 2 – then the value of the adsorbed amount of the dye was greater than zero. In the remaining cases of the tested pH values, the sorption process practically did not take place. Then, the adsorption process was not observed and the amounts of adsorbed dye equalled zero for all three types of sorbents.

The obtained test results also indicate that the largest amounts of the dye were adsorbed on the sorbent generated during the drying process. Under the same experimental conditions, the absorbed charge at pH 2 in the case of the sorbent obtained from drying the post-coagulation sludge was equal to 51.7 mg/g, a slightly lower value was obtained for the sorbent obtained in the oxidation process with H_2O_2 of the sludge (q = 41.8 mg/g) while the lowest value was obtained for the combusted sludge (q = 18.4 mg/g).

3.3. Effect of contact time

In the second stage of the experiments, the influence of the contact time of sorbents with the dye at constant pH conditions, the constant initial concentration of the dye, and the constant amount of sorbents were assessed.

For all sorbents, two different rates of the adsorption process were observed. In general, in the first period of the process, a relatively significant increase in the value of the adsorbed amount of the dye with time was observed. Then the rate of increase of the q_t value with time decreased significantly.

For the dried post-coagulation sludge (Fig. 6), the fastest growth of the amount of adsorbed dye occurred during the first 30 min of contact. A slower rate of the adsorption process was observed between the 30th and 90th min of the process, after which the saturation of the sorbent surface with dye particles was obtained. The value of the adsorbed amount of dye remained constant. In the case of the sludge oxidized with H_2O_2 (Fig. 7), the main increase in q_t value was also observed in the first 30 min of the process, then a much smaller increase in q_t occurred between the 30th and 60th min of the process, after which the value of the amount of adsorbed dye remained relatively constant.

In the case of the combusted sludge (Fig. 8), the fastest increase in the value of the adsorbed amount of dye was obtained in the first 45 min of the process. Next, the q_t value increased slightly in the next 45 min and then remained relatively unchanged until the end of the experiment.

Based on the results of experiments aimed at determining the effect of contact time on the effectiveness of the process, a graph of adsorption efficiency vs. contact time was also made for all tested sorbents (Fig. 9). The highest efficiency of the process was noted for the sorbent made from the dried sludge, while the lowest for the sorbent made from the combusted sludge. In the case of the sorbent produced from the oxidized sludge, the effectiveness of the adsorption process was similar to that of the dried sludge. For example, for a contact time of 120 min, the dye removal was 26.1% and 8.8% for the dried sludge and the combusted sludge, respectively. In the case of the oxidized sludge, the removal rate was 26.0% after 120 min of contact the sorbent with the dye solution.

3.4. Adsorption kinetics

Based on the conducted experiments on the influence of the adsorbent contact time with the dye solution, the parameters of three kinetic models were determined: pseudo-first-order, pseudo-second-order, and intraparticle diffusion. The obtained estimation results indicate that for all three tested sorbents a greater degree of matching to the experimental data was obtained for the pseudo-first-order kinetics model (Table 3). In all cases, both using estimations by minimization of the RMSE and the chi-square values of errors, larger values of R^2 were obtained for the pseudo-first-order kinetic model in comparison with the values obtained for the pseudo-second-order model. Moreover, for all three sorbents, the values of q_e calculated based on the pseudo-first-order kinetics model are more similar to those obtained as a result of the experiments. For example, in the case of dried sludge, the q_e value obtained in the experiments was 91.2 mg/g and the q_e values estimated in the pseudo-first-order model were 93.2 and 93.5 mg/g for the estimation based on RMSE and chi-square, respectively. For comparison, the q_e values obtained (for the same sorbent) based on the pseudo-second-order model were 117.0 and 121.2 mg/g for the estimation based on RMSE and chi-square, respectively. In the case of the other two adsorbents, analogous relationships were noted (Table 3). Therefore, it can be concluded that in the case of the tested adsorbents, in the case of the

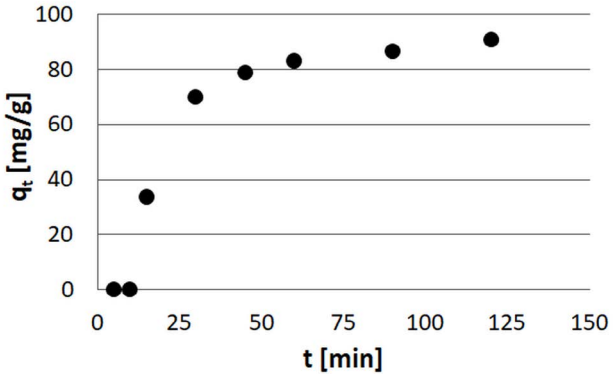

Fig. 7. Effect of contact time for H_2O_2 oxidized sludge.

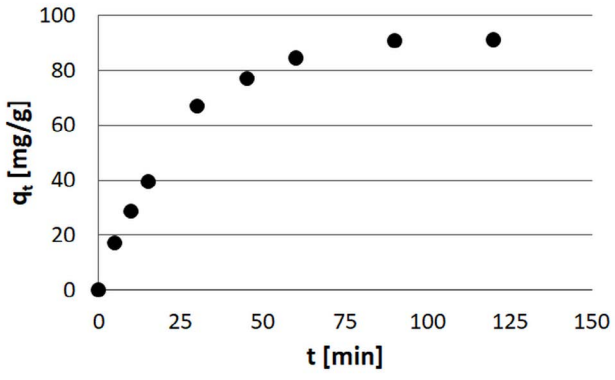

Fig. 6. Effect of contact time for dried sludge.

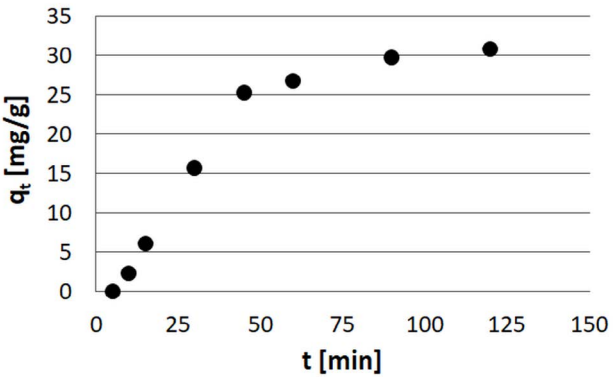

Fig. 8. Effect of contact time for combusted sludge.

adsorption of the Helaktyn Blue F-2R dye, the adsorption took place following the pseudo-first-order kinetics. As the obtained estimation results showed that the fit of the pseudo-second-order kinetic model is smaller, chemical adsorption did not take place. This conclusion is since the pseudo-second-order model is used to describe the kinetics of adsorption when chemical adsorption occurs [27–29].

The dye adsorption process on the adsorbent surface proceeds in several stages. In the first step, the dye molecules move towards the outer surface of the adsorbent. That step of sorption is called film diffusion or outer diffusion. The next step of the sorption process is connected with the transport of dye particles from the external surface into the internal pores of the adsorbent, which process is called intraparticle diffusion or inner diffusion. The last step of the adsorption process takes place when the dye particles are adsorbed on the active sites [30]. Usually, for adsorption, the rate-limiting step is film diffusion or intraparticle diffusion [31]. Therefore, based on the results of the effect of the contact time on the sorption efficiency, the adsorption mechanism was examined by fitting the intraparticle diffusion model to the experimental results.

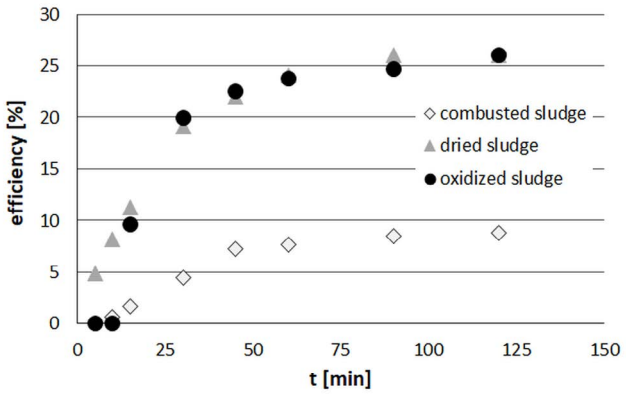

Fig. 9. Process' efficiency.

Based on the graphs of $q_t = f(t^{0.5})$, it can be seen that for all three sorbents two different stages are distinguished (Fig. 10). The first sharpened portion is related to the film diffusion. In the case of dried sludge and oxidized sludge, the film diffusion lasted approximately 30 min. In the case of combusted sludge, this step took 45 min. The second linear portion represents the intraparticle diffusion step of adsorption. This step took 90 min in the case of two tested sorbents (dried sludge and oxidized with H_2O_2 sludge). For the combusted sludge the intraparticle diffusion step lasted approximately 75 min. The ratio of the first step to the second step time for dried sludge and oxidized sludge was 1:3. However, in the case of combusted sludge, this ratio equalled 3:5. In all cases, the second step (intraparticle diffusion) took more time. It may indicate that the rate of the adsorption process will be controlled to a greater extent by the inner diffusion process [30].

In the case of combusted sludge and oxidized sludge, a high degree of model fit to the experimental results was obtained, which is indicated by the obtained R^2 values (Table 4). The lowest R^2 value was obtained for dried sludge (only 0.882). This may indicate that in the case of that sorbent, this kinetic model should not be used to predict the rate of the sorption process. The highest value of the K_{IPD} constant was obtained for the dried sludge and a slightly lower value was obtained for the oxidized sludge. On the other hand, for the combusted sludge, K_{IPD} was almost three times smaller. For all sorbents, the plot does not pass through the origin, which proves that intraparticle diffusion is not only the rate-controlling step [32]. The parameter C is the intercept representative of the boundary layer thickness [33]. The C value gives information about the effect of the boundary layer on the adsorption process. As the value of C increases the thickness of the boundary layer also increases. In that case, the transfer of external mass decreased [23]. In the case of the conducted research, the highest value of C was obtained for oxidized sludge and was 53.379, and a slightly lower value of C was obtained for the dried sludge (46.321). However, the smallest, almost three times

Table 3
Parameters of adsorption kinetics

Type of kinetic model			Type of adsorbent		
			Dried	Combusted	Oxidized with H_2O_2
Estimation based on the minimization of the RMSE value	Pseudo-first-order	q_e	93.2	36.1	97.6
		k_1	0.03907	0.01951	0.02902
		R^2	0.998	0.967	0.930
	Pseudo-second-order	q_e	117.0	53.9	134.4
		k_2	0.00033	0.00026	0.00017
		R^2	0.987	0.952	0.902
Estimation based on the minimization of the chi-square value	Pseudo-first-order	q_e	93.5	42.2	102.8
		k_1	0.03849	0.01423	0.02547
		R^2	0.998	0.940	0.913
	Pseudo-second-order	q_e	121.2	70.6	150.4
		k_2	0.00028	0.00012	0.000122
		R^2	0.984	0.924	0.884

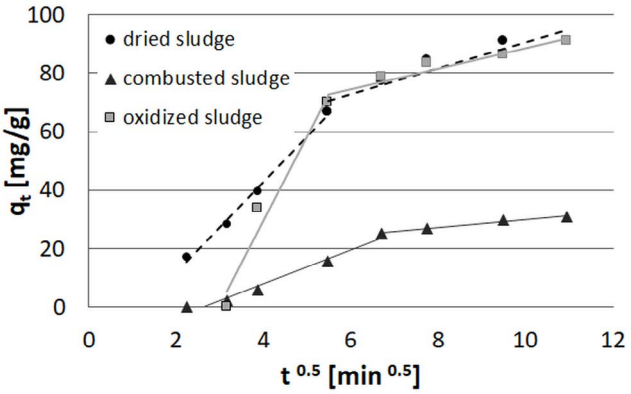

Fig. 10. Intraparticle diffusion plot.

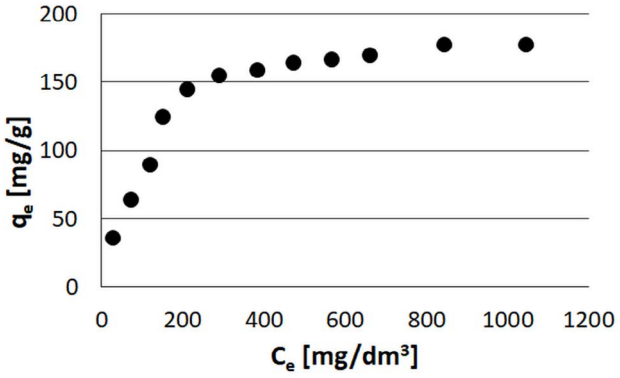

Fig. 11. Adsorption isotherm for dried post-coagulation sludge.

Table 4
Parameters of the intraparticle diffusion model

Parameters	Type of adsorbent		
	Dried	Combusted	Oxidized with H_2O_2
K_{IPD}	4.4337	1.360	3.4303
C	46.321	16.314	53.379
R^2	0.882	0.976	0.927

lower value of C was obtained for the combusted sludge, which was equal to 16.314 (Table 4).

3.5. Sorption isotherm

Based on the results of the third stage of the experiments, a graph of adsorption isotherms $q_e = f(C_e)$ was prepared for each sorbent. The shapes of the obtained curves indicate that for all three sorbents a monolayer process took place in accordance with the IUPAC classification [34] – type I of isotherm occurred. This is evidenced by the presence of a characteristic plateau – after reaching a certain value of the equilibrium concentration C_e, the value of the adsorbed amount of the dye did not change significantly and remained at a relatively constant level. The first type of isotherm according to the IUPAC classification is characteristic of microporous sorbents with a relatively low external surface. In the case of the sorbent obtained from the dried sludge, this boundary value was about 472 mg/dm^3 – then q_e reached the value of 164.1 mg/g and despite a further increase in concentration, the value of q_e did not change significantly (Fig. 11). In the case of the sorbent obtained from the oxidation of the post-coagulation sludge with H_2O_2, the boundary equilibrium concentration was 417 mg/dm^3 and the adsorbed amount of the dye q_e was 91.3 mg/g (Fig. 12). For the sorbent obtained from the combusted post-coagulation sludge, the value of the equilibrium concentration was 205.7 mg/dm^3 – from this equilibrium concentration upwards, the value of q_e remained at the level of 22.1 mg/g (Fig. 13).

Based on the obtained results, it can also be noticed that the greatest sorption properties in relation to the Helaktyn Blue F-2R were obtained for the sorbent prepared from dried post-coagulation sludge. On the other hand, the lowest values were recorded for the sorbent obtained in the process of combusting of this sludge.

To determine the parameters of selected models of two- and three-parameter isotherms, the nonlinear estimation of experiments results (obtained in the third stage of studies) was conducted.

The greatest adjustment of the Freundlich model to the experimental results was obtained for the combusted sludge. In this case, the value of R^2 was 0.933 (RMSE) and 0.931 (χ^2) – Table 5. The smallest adjustment of this model was observed for the dried sludge. The parameter $1/n$ is associated with surface heterogeneity and adsorption intensity. The lower the value of $1/n$, the more heterogeneous the sorbent surface [35,36]. In the studies, the lowest values of $1/n$ were obtained for the combusted sludge (0.147 and 0.154 in the RMSE and χ^2 estimation, respectively), and the highest for the dried sludge (0.310 and 0.346 in the RMSE and χ^2 estimation, respectively). Therefore, the conducted tests indicate a greater heterogeneity of the sorbent surface obtained from the combusted sludge and from oxidized sludge than from the dried sludge. The heterogeneity of the surface means that there are sites with different energy of adsorption values on the surface.

The K_F parameter in the Freundlich model is the isotherm constant associated with relative adsorption capacity [37]. In the case of the conducted experiments, the lowest K_F values were obtained for the combusted sludge, and several times higher K_F values were obtained for the other two types of sorbents (obtained from drying the post-coagulation sludge and from oxidation of the post-coagulation sludge) - Table 5.

The values of exponents in the Sips isotherm model (SP) and exponent in the Toth isotherm model (t) also indicate the heterogeneity of the surface [38,39]. The t and SP parameters usually have a value less than or equal to 1. The lower the exponents value, the more heterogeneous the sorbent surface is. However, when the value of t and SP is equal to 1, then the models of these isotherms turn into the common Langmuir isotherm model of heterogeneity. The value of $t = 1$ and SP = 1 indicates the presence of a homogeneous surface [40]. In the case of the conducted research, the sorbent obtained from the combusted sludge is characterized

Table 5
Values of isotherm parameters obtained during nonlinear estimation

Isotherm model	Parameter	Combusted sludge		Sludge oxidized with H_2O_2		Dried sludge	
		RMSE	χ^2	RMSE	χ^2	RMSE	χ^2
Freundlich	$1/n$	0.147	0.154	0.185	0.195	0.310	0.346
	K_F	9.309	9.009	28.309	26.933	23.004	18.756
	R^2	0.933	0.931	0.893	0.890	0.860	0.849
	Value of error	1.03	0.67	8.13	14.42	18.83	33.33
Langmuir	q_m	22.2	21.4	90.8	90.7	204.5	208.4
	K_L	0.09246	0.17936	0.06633	0.06828	0.00845	0.00785
	R^2	0.848	0.761	0.972	0.971	0.967	0.965
	Value of error	1.75	2.60	4.17	2.86	9.14	7.50
Jovanovic	q_{max}	21.4	20.4	86.0	85.7	173.9	172.9
	K_J	0.0384	0.1721	0.0477	0.0524	0.0073	0.0074
	R^2	0.818	0.470	0.936	0.929	0.994	0.994
	Value of error	2.54	5.03	6.45	7.76	6.80	4.42
Dubinin–Radushkevich	Q_s	21.4	21.3	84.2	79.4	171.1	154.7
	K_{DR}	57.23	2.30	21.37	6.21	1130.5	228.53
	E	0.09	0.47	0.15	0.28	0.02	0.05
	R^2	0.785	0.485	0.873	0.672	0.957	0.691
	Value of error	3.36	5.45	10.27	38.27	14.36	60.31
Sips	q_{mS}	29.8	32.3	93.5	92.9	204.5	208.4
	K_S	0.28258	0.28148	0.09383	0.08672	0.00845	0.00785
	SP	0.394	0.349	0.851	0.885	1.000	1.000
	R^2	0.962	0.961	0.974	0.974	0.967	0.965
	Value of error	0.78	0.41	3.98	2.57	9.14	7.50
Toth	q_{mT}	34.1	39.4	94.5	93.7	204.5	208.4
	K_t	10.61	52.33	0.0933	0.0860	0.0085	0.0079
	t	0.259	0.209	0.779	0.819	1.000	1.000
	R^2	0.959	0.958	0.975	0.975	0.967	0.965
	Value of error	0.81	0.44	3.94	2.53	9.14	7.50

by the greatest heterogeneity of the surface, as the values of t and SP are the lowest. However, in the case of dried sludge, both t and SP are equal to 1, therefore this sludge is characterized by a homogeneous surface (Table 5).

The estimation results for the Langmuir model show that in the case of the oxidized with H_2O_2 sludge and dried sludge, a high degree of matching of this isotherm' model to the experimental results was obtained. This is evidenced by high R^2 values and low RMSE and χ^2 values. In the case of the combusted sludge, the R^2 value is lower than 0.900, which testifies to a relatively low fit of this isotherm model to the experimental results. The value of q_m, obtained as a result of the estimation, is the highest for the dried sludge (204.5 and 208.4 mg/g, calculated based on minimizing the RMSE error and χ^2, respectively). In the case of oxidized with H_2O_2 sludge, the obtained value of sorption capacity q_m was more than half lower than the value obtained for the dried sludge (90.8 and 90.7 mg/g calculated based on the minimization of the RMSE error and χ^2, respectively). The lowest sorption capacity was recorded for the combusted sludge (only 22.2 and 21.4 mg/g calculated based on the minimization of the RMSE error and χ^2, respectively).

The K_L constant in the Langmuir model is related to the free energy of adsorption (dm^3/mg). The highest value of the K_L was obtained for the combusted sludge and the lowest for the dried sludge (Table 3).

The K_J parameter in the Jovanovic model is also related to the free energy of sorption [35,41]. As in the case of the K_L parameter in the Langmuir model, the highest values of K_J were obtained for the combusted sludge and the lowest for the dried sludge. It proves that the adsorption energy of Helaktyn Blue F-2R is higher in the case of the sorbent obtained from the combustion of post-coagulation sludge than in the case of sorbents obtained from oxidized sludge or from dried sludge.

The K_L constant in the Langmuir model, K_S constant in the Sips model, and K_t constant in the Toth model can be regarded as parameters characterizing the affinity of the system [39,40]. The greater the value of these constants, the higher the adsorption affinity is. In the case of the conducted tests, the highest values of these constants were obtained for the combusted sludge, while the lowest was obtained for the dried sludge (Table 5). This proves that in the case of the combusted sludge there are stronger connections between

the dye molecules and the sorbent surface than in the case of other tested sorbents [35]. This may result in a lower susceptibility of the sorbent obtained from the combusted sludge to the desorption process than for the other sorbents.

The sorption capacity was also determined based on the Jovanovic, Dubinin–Radushkevich, Sips, and Toth models. The obtained values were similar to those calculated based on the Langmuir model. The highest sorption capacity was obtained for the dried sludge and it was in the range of 154.7 - 192.5 mg/g (depending on the isotherm model and the estimation method), while the lowest sorbent capacity was obtained for the sorbent obtained from the combustion of post-coagulation sludge – the sorption capacity in the range of 20.4 – 39.4 mg/g (depending on the isotherm model and estimation method). In the case of the sludge oxidized with H_2O_2, the sorption capacity values ranged from 79.4 to 94.5 mg/g (depending on the isotherm model and estimation method).

Based on the Dubinin–Radushkevich model, the sorption energy value was also calculated. The nature of the process – whether physical or chemical adsorption occurs – can be determined based on the value of the energy of sorption [42]. In the studies for all tested sorbents, the values of energy sorption were significantly lower than 8 kJ/mol [43]. Therefore, this indicates that for all sorbents, the process of physical adsorption took place. In such a case, the sorbate particles are bound to the sorbent surface by weak bonds such as van der Waals forces, hydrogen bonding, or hydrophobic interactions [44]. In this case, there was no chemical reaction between the molecules on the surface of the sorbent and the molecules of the dye. One of the main features of physical sorption is that in most cases it is a reversible process, that is, a process of desorption, and thus recovery of valuable substances may take place.

The calculated sorption capacities of the tested three sorbents, as compared to the results obtained in the dye adsorption studies with the use of various sorbents made from waste, show similar values (Table 6). The values of the sorption capacity presented in Table 6 are in a wide range from 3.91 mg/g (for Acid Red 18 sorption onto polar woods) up to 1,133.1 mg/g (when natural clay for Acid Red 88 sorption was used). The monolayer sorption

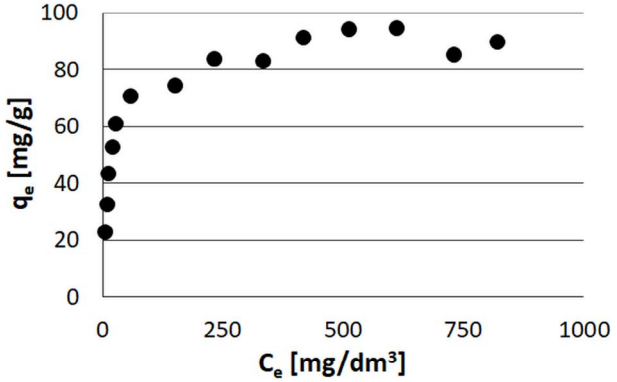

Fig. 12. Adsorption isotherm for oxidized by H_2O_2 post-coagulation sludge.

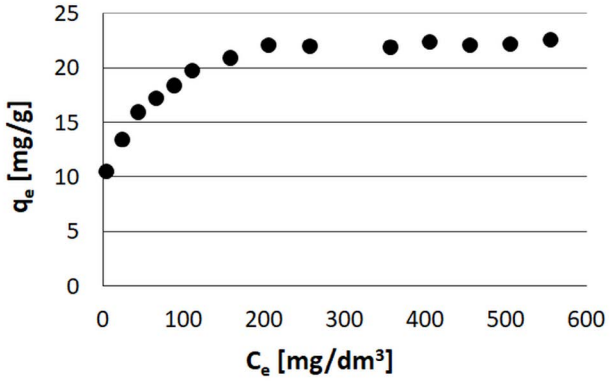

Fig. 13. Adsorption isotherm for combusted post-coagulation sludge.

Table 6
Monolayer sorption capacity for a few different azo dyes sorbed on waste sorbents

Dye	Sorbent	Monolayer sorption capacity q_m (mg/g)	References
Remazol Yellow Gelb 3RS	Activated carbon from olive oil mill residue	50	[45]
Remazol Red RB133	Activated carbon from olive oil mill residue	59.88	[45]
Remazol Schwarz B133	Activated carbon from olive oil mill residue	70.42	[45]
Remazol Yellow Gelb 3RS	Cross-linked chitosan derivatives as sorbents grafted with carboxyl and amide groups	311–928 (depending on the type of adsorbent)	[46]
Brown KROM KGT	Grape pomace as a biosorbent	180.2	[47]
Acid Orange 7	Spent brewers grains	30.5	[48]
Acid Orange 7	Activated carbon powder derived from spent coffee grounds into calcium alginate beads	665.9	[49]
Acid Red 88	Natural clay	1133.1	[50]
Acid Yellow 17	Rambutan *(Nephelium lappaceum)* peel	215.05	[51]
Acid Red 18	Activated carbons prepared from poplar	3.91	[52]
Acid Red 18	Activated carbons prepared from walnut woods	30.3	[52]

capacity value obtained for combusted sludge is comparable to q_m obtained with Acid Red 18 adsorption on activated carbon made from walnut woods and with Acid Orange 7 sorption onto spent brewery grains. In the case of oxidized sludge, the value of sorption capacity is similar to the value obtained during the adsorption of Remazol Schwarz B133 onto activated carbon made from olive oil mill residue. The highest value of the sorption capacity obtained for dried sludge is similar to the capacity obtained in the adsorption studies of Brown KROM KGT dye by grape pomace. It is also similar to the q_m value obtained in the adsorption of Acid Yellow 17 onto Rambutan (*Nephelium lappaceum*) peel.

4. Conclusion

- For all tested sorbents, a strongly acidic condition is required for the effective adsorption process. Only with the use of pH 2.0 of the solution the value of the adsorbed amount of the dye was greater than zero.
- In all cases, a similar effect of the contact time of the sorbent with the dye on the effectiveness of the adsorption process was observed – in the first phase, there was a relatively rapid increase in the value of the adsorbed amount of the dye and the degree of dye removal over time; then in the second phase, the rate of increase in the adsorbed amount of dye in time decreased significantly.
- The analysis of the adsorption kinetics models showed that the pseudo-first-order kinetics model is much better fitted to the experimental results, which indicates physical adsorption rather than chemical adsorption. This is indicated by the value of the R^2 coefficient, the highest values of which were obtained for the pseudo-first-order kinetic model. Moreover, in the case of the pseudo-first-order model, the calculated values are close to the q_e values obtained as a result of the experiments.
- Studies have shown that for all three sorbents, intraparticle diffusion is not the only rate-limiting step in the adsorption process – film diffusion is also important. This is evidenced by the value of parameter *C*, which for all three sorbents was greater than zero – 53.379, 46.321 and 16.314 for dried, combusted and oxidized sludge, respectively.
- The analysis of the intraparticle diffusion model shows that the inner diffusion process is the main factor controlling the rate of the adsorption process - this is indicated by the value of the ratio of the duration of the first linear step to the duration of the second linear step – 1:3 for dried and oxidized sludge, and 3:5 for combusted sludge.
- The shape of the adsorption isotherm curve for all three sorbents is similar to the shape of the I type isotherm according to the IUPAC classification, which is characteristic for microporous sorbents with the relatively low external surface.
- Based on isotherm models, the sorption capacity was determined for each of the sorbents; the highest values were obtained for dried sludge (in the range from 154.7 to 208.4 mg/g – depending on the isotherm model) and the lowest for combusted sludge (in the range from 20.4 to 39.4 mg/g). The obtained values correspond well with the structural characteristics of the tested sorbents. The sorbent made from the dried sludge was characterized by the highest BET surface value (66.4489 m^2/g), while the lowest BET value was measured for the combusted sludge (8.4885 m^2/g).
- The values of the adsorption energy determined from the Dubinin–Radushkevich model indicate that the physical adsorption process occurred – the values for all sorbents were lower than 8 kJ/mol. The obtained results correlate well with the results of the adsorption kinetics analysis, which also indicates that the physical adsorption process has taken place.
- The highest heterogeneity of the sorbent surface was obtained for the combusted sludge and the lowest for the dried sludge. This is evidenced by the values of the parameters: $1/n$ (constant in Freundlich model), SP (exponent in Sips model), and t (exponent in Toth model). In the studies the lowest values of those parameters were obtained for the combusted sorbent.

Acknowledgment

This work was supported by the Ministry of Science and the Higher Education Republic of Poland within statutory funds.

References

[1] M.L. Davis, Water and Wastewater Engineering: Design Principles and Practice, McGraw-Hill Education, New York, 2020.
[2] A.L. Kowal, M. Świderska-Bróż, Water Treatment, PWN, Warszawa, 2003 (in Polish).
[3] M.M. Sozański, Technology of Removal and Disposal of Residuals From Water Treatment, Wydawnictwo Politechniki Poznańskiej, Poznań, 1999 (in Polish).
[4] S. De Carvalho Gomes, J.L. Zhou, X. Zeng, G. Long, Water treatment sludge conversion to biochar as cementitious material in cement composite, J. Environ. Manage., 306 (2022) 114463, doi: 10.1016/j.jenvman.2022.114463.
[5] O. Gencel, S.M.S. Kazmi, M.J. Munir, M. Sutcu, E. Erdogmus, A. Yaras, Feasibility of using clay-free bricks manufactured from water treatment sludge, glass, and marble wastes: an exploratory study, Constr. Build. Mater., 298 (2021) 123843, doi: 10.1016/j.conbuildmat.2021.123843.
[6] E. Erdogmus, M. Harja, O. Gencel, M. Sutcu, A. Yaras, New construction materials synthesized from water treatment sludge and fired clay brick wastes, J. Build. Eng., 42 (2021) 102471, doi: 10.1016/j.jobe.2021.102471.
[7] A. Benlalla, M. Elmoussaouiti, M. Dahhou, M. Assafi, Utilization of water treatment plant sludge in structural ceramics bricks, Appl. Clay Sci., 118 (2015) 171–177.
[8] S.D.C. Gomes, J.L. Zhou, W. Li, F. Qu, Recycling of raw water treatment sludge in cementitious composites: effects on heat evolution, compressive strength and microstructure, Resour. Conserv. Recycl., 161 (2020) 104970, doi: 10.1016/j.resconrec.2020.104970.
[9] H. Zeng, Y. Yu, F. Wang, J. Zhang, D. Li, Arsenic(V) removal by granular adsorbents made from water treatment residuals materials and chitosan, Colloids Surf., A, 585 (2020) 124036, doi: 10.1016/j.colsurfa.2019.124036.
[10] K.C. Makris, D. Sarkar, R. Datta, Aluminum-based drinking-water treatment residuals: a novel sorbent for perchlorate removal, Environ. Pollut., 140 (2006) 9–12.
[11] C. Liu, Z. Tang, Y. Chen, S. Su, W. Jiang, Characterization of mesoporous activated carbons prepared by pyrolysis of sewage sludge with pyrolusite, Bioresour. Technol., 101 (2010) 1097–1101.
[12] K. Björklund, L.Y. Li, Adsorption of organic stormwater pollutants onto activated carbon from sewage sludge, J. Environ. Manage., 197 (2017) 490–497.

[13] F. Rozada, L.F. Calvo, A.I. García, J. Martín-Villacorta, M. Otero, Dye adsorption by sewage sludge-based activated carbons in batch and fixed-bed systems, Bioresour. Technol., 87 (2003) 221–230.
[14] B. Pieczykolan, I. Płonka, Application of excess activated sludge as waste sorbent for dyes removal from their aqueous solutions, Ecol. Chem. Eng. S, 26 (2019) 773–784.
[15] Z. Berizi, S.Y. Hashemi, M. Hadi, A. Azari, A.H. Mahvi, The study of non-linear kinetics and adsorption isotherm models for Acid Red 18 from aqueous solutions by magnetite nanoparticles and magnetite nanoparticles modified by sodium alginate, Water Sci. Technol., 74 (2016) 1235–1242.
[16] I. Ali, S. Afshinb, Y. Poureshgh, A. Azari, Y. Rashtbari, A. Feizizadeh, A. Hamzezadeh, M. Fazlzadeh, Green preparation of activated carbon from pomegranate peel coated with zero-valent iron nanoparticles (nZVI) and isotherm and kinetic studies of amoxicillin removal in water, Environ. Sci. Pollut. Res., 27 (2020) 36732–36743.
[17] Reactive Blue 81, (n.d.).
[18] A. Berrazoum, R. Marouf, F. Ouadjenia, J. Schott, Bioadsorption of a reactive dye from aqueous solution by municipal solid waste, Biotechnol. Rep., 7 (2015) 44–50.
[19] P. Wronski, J. Surmacki, H. Abramczyk, A. Adamus, M. Nowosielska, W. Maniukiewicz, M. Kozanecki, M. Szadkowska-Nicze, Surface, optical and photocatalytic properties of silica-supported TiO_2 treated with electron beam, Radiat. Phys. Chem., 109 (2015) 40–47.
[20] S. Lagergren, Zur theorie der sogenannten adsorption geloster stoffe, K. Sven. Vetenskapsakademiens. Handl., 24 (1898) 1–39.
[21] Y.S. Ho, G. McKay, Pseudo-second-order model for sorption processes, Process Biochem., 34 (1999) 451–465.
[22] W.J. Weber, J.C. Morris, Kinetics of adsorption on carbon from solution, J. Sanit. Eng. Div., 89 (1963) 31–59.
[23] A.L. Prasad, T. Santhi, S. Manonmani, Recent developments in preparation of activated carbons by microwave: Study of residual errors, Arabian J. Chem., 8 (2015) 343–354.
[24] A.B.D. Nandiyanto, R. Oktiani, R. Ragadhita, How to read and interpret FTIR spectroscope of organic material, Indones. J. Sci. Technol., 4 (2019) 97–118.
[25] A. Rajca, W. Zieliński, E. Al., Spectroscopic Methods and Their Application to the Identification of Organic Compounds, Wydawnictwo Naukowo-Techniczne, Warsaw, 1995 (in Polish).
[26] R.M. Silverstein, G.C. Bassler, T. Morrill, Chapter 3: Infrared Spectrometry, Spectrom. Identif. Org. Compd., 5th ed., John Wiley & Sons, New York, 1991, pp. 91–164.
[27] T. Lou, X. Yan, X. Wang, Chitosan coated polyacrylonitrile nanofibrous mat for dye adsorption, Int. J. Biol. Macromol., 135 (2019) 919–925.
[28] F. Fadzail, M. Hasan, Z. Mokhtar, N. Ibrahim, Removal of naproxen using low-cost *Dillenia Indica* peels as an activated carbon, Mater. Today:. Proc., 57 (2022) 1108–1115.
[29] R.K. Sharma, R. Kumar, A.P. Singh, Metal ions and organic dyes sorption applications of cellulose grafted with binary vinyl monomers, Sep. Purif. Technol., 209 (2019) 684–697.
[30] B. Singha, S.K. Das, Biosorption of Cr(VI) ions from aqueous solutions: kinetics, equilibrium, thermodynamics and desorption studies, Colloids Surf., B, 84 (2011) 221–232.
[31] M.H. Kalavathy, T. Karthikeyan, S. Rajgopal, L.R. Miranda, Kinetic and isotherm studies of Cu(II) adsorption onto H_3PO_4-activated rubber wood sawdust, J. Colloid Interface Sci., 292 (2005) 354–362.
[32] W. Konicki, M. Aleksandrzak, D. Moszyński, E. Mijowska, Adsorption of anionic azo-dyes from aqueous solutions onto graphene oxide: equilibrium, kinetic and thermodynamic studies, J. Colloid Interface Sci., 496 (2017) 188–200.
[33] B. Cheknane, F. Zermane, M. Baudu, O. Bouras, J.P. Basly, Sorption of basic dyes onto granulated pillared clays: thermodynamic and kinetic studies, J. Colloid Interface Sci., 381 (2012) 158–163.
[34] M. Muttakin, S. Mitra, K. Thu, K. Ito, B. Saha, Theoretical framework to evaluate minimum desorption temperature for IUPAC classified adsorption isotherms, Int. J. Heat Mass Transfer, 122 (2018) 795–805.
[35] S. Li, L. Zhong, H. Wang, J. Li, H. Cheng, Q. Ma, Process optimization of polyphenol oxidase immobilization: Isotherm, kinetic, thermodynamic and removal of phenolic compounds, Int. J. Biol. Macromol., 185 (2021) 792–803.
[36] K.Y. Foo, B.H. Hameed, Insights into the modeling of adsorption isotherm systems, Chem. Eng. J., 156 (2010) 2–10.
[37] M.L.F.A. De Castro, M.L.B. Abad, D.A.G. Sumalinog, R.R.M. Abarca, P. Paoprasert, M.D.G. de Luna, Adsorption of methylene blue dye and Cu(II) ions on EDTA-modified bentonite: isotherm, kinetic and thermodynamic studies, Sustainable Environ. Res., 28 (2018) 197–205.
[38] M. Brdar, M. Šćiban, A. Takači, T. Došenović, Comparison of two and three parameters adsorption isotherm for Cr(VI) onto kraft lignin, Chem. Eng. J., 183 (2012) 108–111.
[39] A. Sarkar, B. Paul, Analysis of the performance of zirconia-multiwalled carbon nanotube nanoheterostructures in adsorbing As(V) from potable water from the aspects of physical chemistry with an emphasis on adsorption site energy distribution and density functional theory calculations, Microporous Mesoporous Mater., 302 (2020) 110191, doi: 10.1016/j.micromeso.2020.110191.
[40] S. Ullah, M.A. Bustam, A.G. Al-Sehemi, M.A. Assiri, F.A. Abdul Kareem, A. Mukhtar, M. Ayoub, G. Gonfa, Influence of post-synthetic graphene oxide (GO) functionalization on the selective CO_2/CH_4 adsorption behavior of MOF-200 at different temperatures; an experimental and adsorption isotherms study, Microporous Mesoporous Mater., 296 (2020) 110002, doi: 10.1016/j.micromeso.2020.110002.
[41] Z. Lu, C. Huangfu, Y. Wang, H. Ge, Y. Yao, P. Zou, G. Wang, H. He, H. Rao, Kinetics and thermodynamics studies on the BMP-2 adsorption onto hydroxyapatite surface with different multi-morphological features, Mater. Sci. Eng. C, 52 (2015) 251–258.
[42] L. Mihaly-Cozmuta, A. Mihaly-Cozmuta, A. Peter, C. Nicula, H. Tutu, D. Silipas, E. Indrea, Adsorption of heavy metal cations by Na-clinoptilolite: equilibrium and selectivity studies, J. Environ. Manage., 137 (2014) 69–80.
[43] S. Kasap, H. Tel, S. Piskin, Preparation of TiO_2 nanoparticles by sonochemical method, isotherm, thermodynamic and kinetic studies on the sorption of strontium, J. Radioanal. Nucl. Chem., 289 (2011) 489–495.
[44] M.T. Yagub, T.K. Sen, S. Afroze, H.M. Ang, Dye and its removal from aqueous solution by adsorption: a review, Adv. Colloid Interface Sci., 209 (2014) 172–184.
[45] A. Pala, P. Galiatsatou, E. Tokat, H. Erkaya, C. Israilides, D. Arapoglou, The use of activated carbon from olive oil mill residue, for the removal of colour from textile wastewater, European Water, 13 (2006) 29–34.
[46] G.Z. Kyzas, N.K. Lazaridis, Reactive and basic dyes removal by sorption onto chitosan derivatives, J. Colloid Interface Sci., 331 (2009) 32–39.
[47] A.P. de Oliveira, A.N. Módenes, M.E. Bragião, C.L. Hinterholz, D.E.G. Trigueros, I.G. de O. Bezerra, Use of grape pomace as a biosorbent for the removal of the Brown KROM KGT dye, Bioresour. Technol. Rep., 2 (2018) 92–99.
[48] J.P. Silva, S. Sousa, J. Rodrigues, H. Antunes, J.J. Porter, I. Gonçalves, S. Ferreira-Dias, Adsorption of Acid Orange 7 dye in aqueous solutions by spent brewery grains, Sep. Purif. Technol., 40 (2004) 309–315.
[49] K.W. Jung, B.H. Choi, M.J. Hwang, T.U. Jeong, K.H. Ahn, Fabrication of granular activated carbons derived from spent coffee grounds by entrapment in calcium alginate beads for adsorption of Acid Orange 7 and methylene blue, Bioresour. Technol., 219 (2016) 185–195.
[50] S.T. Akar, R. Uysal, Untreated clay with high adsorption capacity for effective removal of CI Acid Red 88 from aqueous solutions: batch and dynamic flow mode studies, Chem. Eng. J., 162 (2010) 591–598.
[51] V.O. Njoku, K.Y. Foo, M. Asif, B.H. Hameed, Preparation of activated carbons from Rambutan (*Nephelium lappaceum*) peel by microwave-induced KOH activation for Acid Yellow 17 dye adsorption, Chem. Eng. J., 250 (2014) 198–204.
[52] B. Heibati, S. Rodriguez-Couto, M.A. Al-Ghouti, M. Asif, I. Tyagi, S. Agarwal, V.K. Gupta, Kinetics and thermodynamics of enhanced adsorption of the dye AR 18 using activated carbons prepared from walnut and poplar woods, J. Mol. Liq., 208 (2015) 99–105.